Surfactant Assisted Processing of Carbon Nanotube/ Polypropylene Composites: Impact of Surfactants on the Matrix Polymer

Julius Rausch, Rong-Chuan Zhuang, Edith Mäder

Department of Composites, Leibniz Institute of Polymer Research Dresden, Dresden 01069, Germany

Received 23 December 2008; accepted 15 March 2009
DOI 10.1002/app.32194
Published online 27 April 2010 in Wiley InterScience (www.interscience.wiley.com).

ABSTRACT: Multiwalled carbon nanotubes (MWCNT) were dispersed in presence of various surfactants and introduced into isotactic polypropylene (PP) via melt blending. The effect of the surfactants on the crystallization and mechanical properties was studied on the injection molded specimens by isothermal differential scanning calorimetry and tensile tests, respectively. The results reveal that the presence of surfactants affects the mechanical and thermal properties of the nanocomposite. This information is supported by thermogravimetric analysis of the surfactants to examine their behavior at temperatures relevant for the processing of PP. In addition, they have to be taken into account as a third phase between the MWCNT and polymeric matrix, affecting the crystallization and failure behavior of PP or causing the formation of pores at elevated temperatures. © 2010 Wiley Periodicals, Inc. J Appl Polym Sci 117: 2583–2590, 2010

Key words: polypropylene (PP); nanocomposites; surfactants; differential scanning calorimetry (DSC)

INTRODUCTION

Since the discovery of carbon nanotubes (CNT) in the early 1990s,[1] a considerable effort towards the development of novel CNT-based materials has been made. CNT are a promising material for manifold applications related to their unique set of physical properties.[2] Consequently, in the field of polymer materials, numerous attempts have been made to exploit their potential as a filler material to enhance mechanical properties of polymers[3] or to tailor the electrical conductivity of materials.[4–6] Generally, for mechanical reinforcement homogeneous distribution and exfoliation of the CNT as well as favorable interfacial interaction with the polymeric matrix are regarded as key issues. However, despite intensive research on CNT nanocomposites, the incorporation of CNT into polymers in terms of their homogeneous distribution and exfoliation remains a challenge, as pristine CNT tend to form bundles due to van der Waals interactions, which were estimated to be in the order of 500 eV/μm for singlewalled CNT (SWCNT).[7]

Several approaches have been proposed for the preparation of CNT-based nanocomposites depending on the intended application. As it is desirable to employ established processing methods for producing thermoplastic nanocomposites, the preparation of master batches in combination with subsequent melt compounding has proved its applicability for processing CNT nanocomposites on the bigger scale.[8,9] Using this approach, the exfoliation of the CNT is achieved mechanically by shear forces acting during the compounding process in the extruder. However, good results regarding the distribution homogeneity and exfoliation of CNT in the matrix have been reported as well for nanocomposites involving a predispersion of the CNT achieved by mixing or sonication.[10–13] Colloidally stable and highly exfoliated CNT can be incorporated into thermoplastic resins, e.g. by latex technology.[14] Despite the ease of dispersing CNT in aqueous media in the presence of different surfactants or polymers,[15] this approach is hardly applicable for processing of nanocomposites on the bigger scale and is therefore restricted to films, smaller batches or more specific applications as for instance the incorporation of CNT into fibre sizing formulations. For the latter application, it has been demonstrated that smallest amounts of CNT located in the interphase of glass fibre based composites can enhance their mechanical properties.[16,17]

Sonication in presence of surfactants has been widely used to prepare aqueous CNT dispersions

Correspondence to: E. Mäder (emaeder@ipfdd.de).
Contract grant sponsors: Deutsche Forschungsgemeinschaft (DFG) Collaborative Research Centre.

with a high degree of exfoliation. Local shear throughout sonication frays the bundled CNT providing additional sites for surfactant adsorption. Taking those places as starting points for the individualization of the bundled CNT, more surfactant molecules adsorb at those sites, thus gradually propagating the detachment of single CNT from the bundle, ending up in individualized and surfactant-covered CNT as proposed by Strano et al.[18]

If it comes to the evaluation of the dispersion quality of CNT dispersed in aqueous media, the application of UV-vis spectroscopy provides a straightforward method to quantify the degree of CNT exfoliation,[12] as CNT are known to absorb in the ultraviolet region.[19] Hence, absorbance of CNT at a specific wavelength can be related to the degree of exfoliation of CNT in aqueous media. With increasing sonication time, the absorbance is reported to follow a characteristic pattern, starting off from zero and rapidly increasing before showing a plateau-like behavior, indicating that a state of dynamic equilibrium has reached and further sonication does not improve the degree of CNT exfoliation.[10] If CNT are dispersed in presence of surfactants, the stability of the colloidal CNT is achieved by adsorption of the surfactant molecules onto the CNT. Various micelle structures have been proposed. In the case of SWCNT dispersed in sodium dodecyl sulfate (SDS), cylindrical structures as well as hemimicelles were suggested,[20] whereas other work proposed random adsorption of the surfactant molecules on the CNT surface, depending on the concentration of surfactant used.[15,21]

Independent of the type of micelle and nature of surfactant, the exfoliated CNT are assumed to be fully covered by surfactant molecules if the CNT/surfactant weight ratio is adjusted accordingly.[22] In the case of nanocomposites this means that a third phase on the nanometre scale besides reinforcing agent and matrix material has to be taken into account. Few studies can be found in literature using the surfactant assisted dispersion of CNT for their subsequent incorporation into bulk matrices. Gong et al.[23] employed a nonionic surfactant to disperse CNT before they were added to an epoxy resin before curing. In a more recent work, Miltner et al.[14] studied the thermal properties of CNT/PP nanocomposites prepared by latex technology dispersing the CNT in presence of SDS. However, those studies rather demonstrate the enhanced dispersion quality due to the use of surfactants than discussing the specific interactions between the surfactant-covered CNT and matrix polymer. Especially in the case of semicrystalline thermoplastic resins, the reinforcing effect of CNT is assumed to be strongly related to the ability of the CNT to alter the morphology in their vicinity.[9] The presence of different surfactants in the CNT/matrix interface possibly affects the nucleation ability of the CNT, which would be reflected in a change of mechanical properties. Furthermore, the chemical nature of surfactants is likely to influence the dispersion process of the CNT during melt processing depending on the polarity of the thermoplastic resin.

To achieve a better understanding of those issues, the scope of this work is to study the effect of different surfactants in the CNT/matrix interface using PP as a matrix.

EXPERIMENTAL

Sample preparation

Commercially available carboxyl functionalized MWCNT (NC3101, Nanocyl S.A., Belgium) were dispersed in aqueous solution of various surfactants, namely sodium dodecyl sulfate (SDS, melting point (mp) = 206°C), polyethylene glycol octadecyl ether (Brij76, mp = 37–39°C), both provided by Sigma Aldrich, and hexadecyltrimethylammonium bromide (CTAB, Merck, mp = 250°C). All samples had a constant MWCNT/surfactant weight ratio of 1/3 and underwent equal batch-wise sonication employing a tip sonicator (Hielscher UP200S) at constant output power of 180 W equipped with a cylindrical sonotrode (3 mm) for 180 min. Throughout sonication the beaker with the suspended MWCNT was cooled in a water bath.

After sonication the MWCNT dispersions were mixed with granules of PP (HG 455FB, Borealis). The water was slowly evaporated leaving granules densely covered by the predispersed MWCNT upon magnetic stirring at 50°C. The relative weight of MWCNT with regard to the thermoplastic resin was thereby adjusted to 1 wt %. The samples based on PP/surfactant without MWCNT were prepared by dissolving the surfactant in deionized water, mixing it with the granules followed by evaporation of the water as mentioned above. Additionally, one system containing MWCNT was prepared without any predispersion or addition of surfactants, but mixing the MWCNT in their powdery, as-delivered form with the PP granules. Table I summarizes the samples prepared. Before compounding, the granules of all samples were dried at 50°C for 3 h in a vacuum oven.

Compounding was conducted on a corotating twin-screw extruder (Haake Rheomex PTW 16/25DW) at 100 rpm. The barrel temperature was adjusted in between 180 and 220°C. A second processing step comprised the injection molding of S2 tensile bars on a Boy 22A HV with a screw diameter of 18 mm and l/d-ratio of 20. The adjusted barrel temperatures ranged from 190 to 225°C.

TABLE I
Samples Prepared for Characterization

Polymer	Surfactant	MWCNT
PP	–	–
PP	–	NC3151
PP	SDS	–
PP	SDS	NC3151
PP	Brij76	–
PP	Brij76	NC3151
PP	CTAB	–
PP	CTAB	NC3151

Characterization

At the end of sonication, samples of the dispersions were taken and diluted 200 times with deionized water before recording UV-vis spectra (PerkinElmer Lambda 800). All spectra were captured in the wavelength region between 205 and 800 nm using a blank filled with deionized water.

The isothermal crystallization was studied by differential scanning calorimetry (DSC; Q 2000, TA Instruments) under nitrogen atmosphere. The samples were heated from room temperature to 205°C and maintained at this temperature for 5 min to account for their thermal prehistory. Next, the samples were cooled to the isothermal crystallization temperature of 140°C. After crystallization was completed, the samples were cooled to ambient temperature. Applied heating and cooling rates were 50 K/min and 20 K/min, respectively.

Thermogravimetric analysis (TGA) under air purge was performed on the surfactants using a Q 500 (TA Instruments).

The injection molded tensile bars were cryofractured and the morphology of the fractured surfaces was characterized by scanning electron microscopy (Zeiss ULTRA plus). All samples were coated with a platinum layer of about 6 nm.

Characterization of tensile properties was conducted on a Zwick 1456 (Zwick GmbH) following ISO 527-2, using S2 tensile bars and a test velocity of 10 mm/min.

RESULTS AND DISCUSSION

Effect of surfactant assisted predispersion of MWCNT on crystallization of PP

As it is intended to investigate the suitability of various surfactants for the preparation of PP/MWCNT nanocomposites emphasizing on the characterization of their impact on the matrix polymer, it is of importance that the MWCNT are predispersed to a similar degree in all systems. Thus it can be assured that differences observed by characterization of injection molded samples are related to the corresponding surfactant and its influence on the processing of the nanocomposites, assuming that the conformation of individualized MWCNT by adsorption of surfactant molecules onto the MWCNT in the aqueous systems is preserved upon evaporation of water. Figure 1 shows the UV-vis spectra of the MWCNT dispersed in presence of the surfactants. Relating the maximum absorbance to the degree of exfoliation for the dispersed MWCNT[12] a similar degree of exfoliation for the three different systems is observed, although slightly lower maximum absorbance value is obtained for CTAB/MWCNT than those for the systems using SDS and Brij76, respectively. The differences in the potential of the surfactants for dispersing MWCNT are related to the nature of the used surfactants and the resulting specific interactions with the MWCNT described elsewhere.[24] However, as the deviation in maximum absorbance shown in the inset of Figure 1 is small, it can be assumed that a similar starting condition for all systems is provided.

The morphology of semicrystalline thermoplastics is known to affect the mechanical properties to a great extent. Numerous studies have investigated the effect of CNT on the crystallization of PP and it is widely accepted that CNT act as nucleating agents for PP.[14,25–31] The intention of this study is not to add one more set of affirmative results of the nucleating ability of CNT in PP, rather the effect of the surfactant on the crystallization of the nanocomposites is of interest. Bearing in mind the high specific surface area of CNT and the fact that individualized CNT are covered with surfactant molecules upon the sonication process in presence of surfactants, the surfactant molecules are expected to be mainly located in the CNT/PP interface.

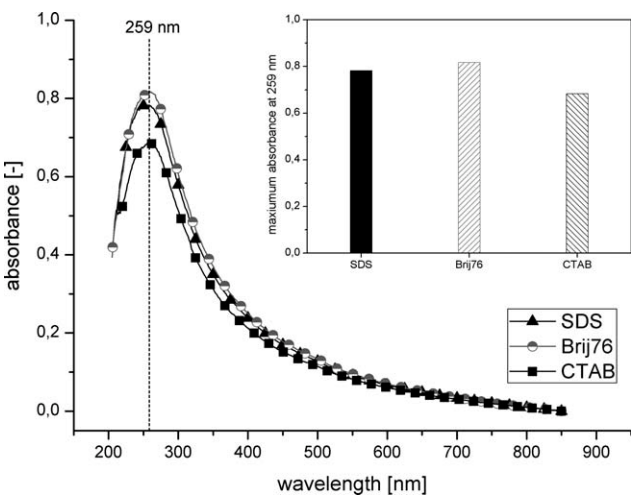

Figure 1 UV-vis spectra of MWCNT dispersed in presence of the different surfactants after 180 min of sonication. Inset figure: Maximum absorbance of dispersed MWCNT at 259 nm.

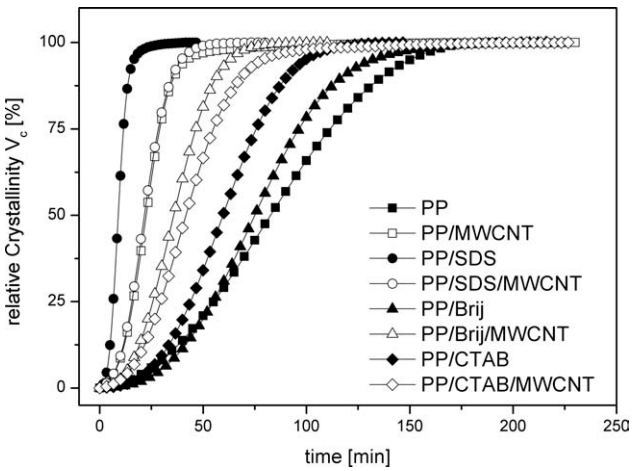

Figure 2 Evolution of relative crystallinity for isothermal crystallization at 140°C.

Figure 2 shows the evolution of the relative crystallinity with crystallization time for neat PP and the PP/surfactant as well as the PP/surfactant/MWCNT systems. It can be seen that the crystallization process of the neat PP is the slowest one. The addition of surfactants results in accelerated crystallization of the PP. Hence, all surfactants serve as nucleating agents, however, to a varying extent. In detail, Brij76 and CTAB cause a modest acceleration of crystallization, the addition of SDS to PP leads to a pronounced change of the crystallization kinetics. One reason for the difference in the influence of surfactants on the crystallization kinetics is related to their different melting points. Besides volume fraction and surface area, nucleating agents are commonly used in the solid state rather than in the molten state to provide interfacial area for the primary crystallization. In the case of PP and the surfactants used this means that (i) due to its high melting point and high polarity CTAB does not melt during compounding and DSC investigation and preserves its structure forming big agglomerates as observed by optical light microscopy and SEM (results not shown). Due to its poor distribution in the PP matrix only little surface area is available for inducing crystallization of PP; (ii) Brij76 can homogenously distribute in the matrix in the course of compounding owing to its low melting point and nonionic character. However, the contribution to the nucleation of PP is very modest as its melting point is considerably lower than the crystallization temperature of PP; (iii) SDS has a higher melting point than neat PP but it is lower than the compounding temperature, as a result, SDS has a better distribution in PP in comparison to CTAB but worse than Brij76. More important, SDS has a melting point above the crystallization temperature of PP, therefore SDS can be assumed to be in the solid when it comes to the crystallization of PP providing sites for heterogeneous nucleation.

Taking a closer look at the systems containing MWCNT, it can be observed that the predispersion of the MWCNT in presence of surfactants leads to a further reduction in the crystallization half-time, $t_{0.5}$, of the PP/Brij76/MWCNT and the PP/CTAB/MWCNT system, respectively (cf. Table II). However, in the case of SDS the crystallization of the system containing MWCNT is slower than that of the one without MWCNT, but still considerably faster than the crystallization of other surfactant-based systems. Interestingly, the sample containing pristine MWCNT without predispersion crystallizes faster than the PP/Brij76/MWCNT and the PP/CTAB/MWCNT ones, showing similar crystallization kinetics as the PP/SDS/MWCNT sample.

For analysis of the isothermal crystallization kinetics the Avrami equation[32] assumes that the relative degree of crystallinity V_c is related to the crystallization time t by

$$1 - V_c = \exp(-k\, t^n) \tag{1}$$

with k being the crystallization rate constant and n the Avrami exponent. The latter one is related to the nature of nucleation as well as the growth of the crystallites. Figure 3 depicts the Avrami plots on the basis of the relative crystallinities shown in Figure 2. A conversion range of $5\% < V_c < 60\%$ was chosen to fit the experimental data, assuring high coefficients

TABLE II
Crystallization Half-Time $t_{0,5}$ and Avrami Parameters n and k for Isothermal Crystallization at 140°C

Sample	$t_{0,5}$ [min]	n	k [min]$^{-n}$	Coefficient of correl.
PP	82,6	2,1	7,31E-05	0,99912
PP/MWCNT	22,5	2,5	3,05E-04	0,99732
PP/SDS	9,0	2,8	1,52E-03	0,99957
PP/SDS/MWCNT	21,6	2,5	3,04E-04	0,99855
PP/Brij	75,0	2,8	4,43E-06	0,99994
PP/Brij/MWCNT	35,8	2,6	5,77E-05	0,99995
PP/CTAB	59,6	2,8	6,44E-06	0,99988
PP/CTAB/MWCNT	41,7	2,5	6,42E-05	0,99976

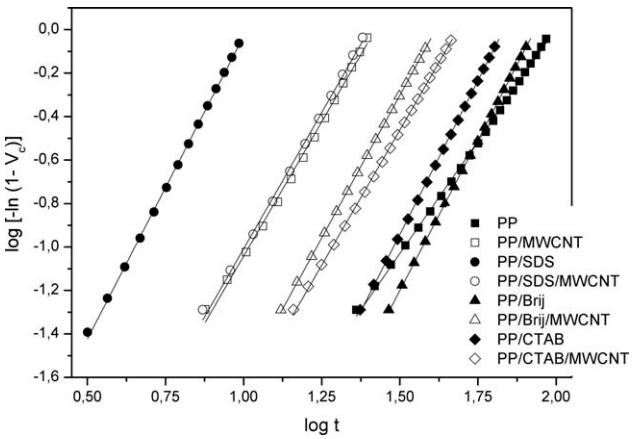

Figure 3 Avrami plots for neat PP, PP/surfactant, and PP/surfactant/MWCNT systems.

of correlation of >0.99.[33] The slopes of the Avrami plots and the intercepts with the ordinate provide the Avrami parameters n and k, respectively. Table II summarizes the values for $t_{0.5}$ as well as the Avrami parameters n and k. Comparing the values for n, the lowest value of the Avrami exponent can be found for neat PP (2.1), whereas all other samples have n-values ranging from 2.5 to 2.8. This indicates that the nucleation process is similar for all samples apart from the neat PP. This is not surprising as the nucleating ability of the surfactants is already reflected in the dependence of relative crystallinity on crystallization time. The listed values for $t_{0.5}$ in Table II allow to derive conclusions whether the presence of the adsorbed surfactant molecules affects the nucleation ability of the MWCNT or not. It becomes evident from the DSC data that the surfactants themselves as well as the pristine MWCNT act as nucleating agents for PP. However, the pristine MWCNT cause a faster crystallization than all PP/surfactant systems with the exception of PP/SDS. Thus it is not surprising to observe a further reduction in the crystallization half-time for the PP/Brij76/MWCNT and PP/CTAB/MWCNT samples compared with the same systems without MWCNT. The shortest $t_{0.5}$-time was observed for the system of PP with pristine MWCNT, indicating that the predispersion of the MWCNT in presence of Brij76 and CTAB lowers the nucleating ability of the MWCNT. Bearing in mind that the mechanism for dispersion and stabilization of MWCNT in aqueous media and presence of surfactants is based on the adsorption of the surfactant molecules onto the MWCNT surface, most of the surfactant molecules are located in the PP/MWCNT interface, where they affect the nucleation of the PP and obviously hamper its nucleation induced by the MWCNT. This can also account for the slower evolution of crystallization of PP/SDS/MWCNT in comparison to PP/SDS. The MWCNT are coated with SDS with its polar head group pointing outwards and being partly present in agglomerates, thus their effective surface area for inducing nucleation of PP is significantly reduced. Additionally, a considerable amount of the SDS is enclosed in the MWCNT agglomerates not contributing to the nucleation of PP.

The results indicate that no simple superposition of the contributions to nucleation by the surfactants and MWCNT is taking place as systems containing the surfactant predispersed MWCNT are partly slower than the one with pristine MWCNT or PP/SDS. In case of an addition of the two contributions to the nucleation of the PP, the systems with the predispersed MWCNT should result in accelerated, which can not be observed. Generally, in case of heterogeneous nucleation, the crystallization of a polymer is affected by the provided surface area of the nucleating agent and the comparability of the results is only assured for a similar state of dispersion, i.e. equal surface area of the nucleating agent. For CNT this is reflected in the fact that for similar filler weight fractions and state of dispersion a higher nucleation efficiency of SWCNT compared with MWCNT was observed.[14] Those findings are related to the higher specific surface area of the SWCNT, whereas due to tubular stacking of the different walls in MWCNT their effective surface area is decreased. In this study, for the given set of samples containing MWCNT, the pristine MWCNT result in the fastest crystallization although showing lower dispersion homogeneity, as evidenced by SEM (cf. Fig. 4) and the mechanical characterization (cf. Fig. 6), compared with the samples containing the MWCNT predispersed in presence of surfactants. Considering this issue, the observed differences in the nucleation or crystallization half-time are likely to be even more pronounced if an equal surface area for nucleation were provided for all samples.

Fractured surfaces of PP nanocomposites

Fractured surfaces provide valuable information on the distribution of nanofillers within the matrix material, their agglomerate size, and the fracture mechanism of the sample. Nonetheless, a mere judgement of the state of dispersion of CNT by means of SEM can rarely provide a comprehensive picture of the distribution homogeneity. However, distinct differences in the investigated fractured surfaces are revealed and representative SEM micrographs are shown in Figure 4. The samples are taken from middle of the tensile bars with the fracture plane being perpendicular to the direction of injection molding.

Figure 4(a) shows the fractured surface of the nanocomposite containing pristine MWCNT without any predispersion. The edge of a bigger agglomerate can be seen and the loose appearance of the MWCNT

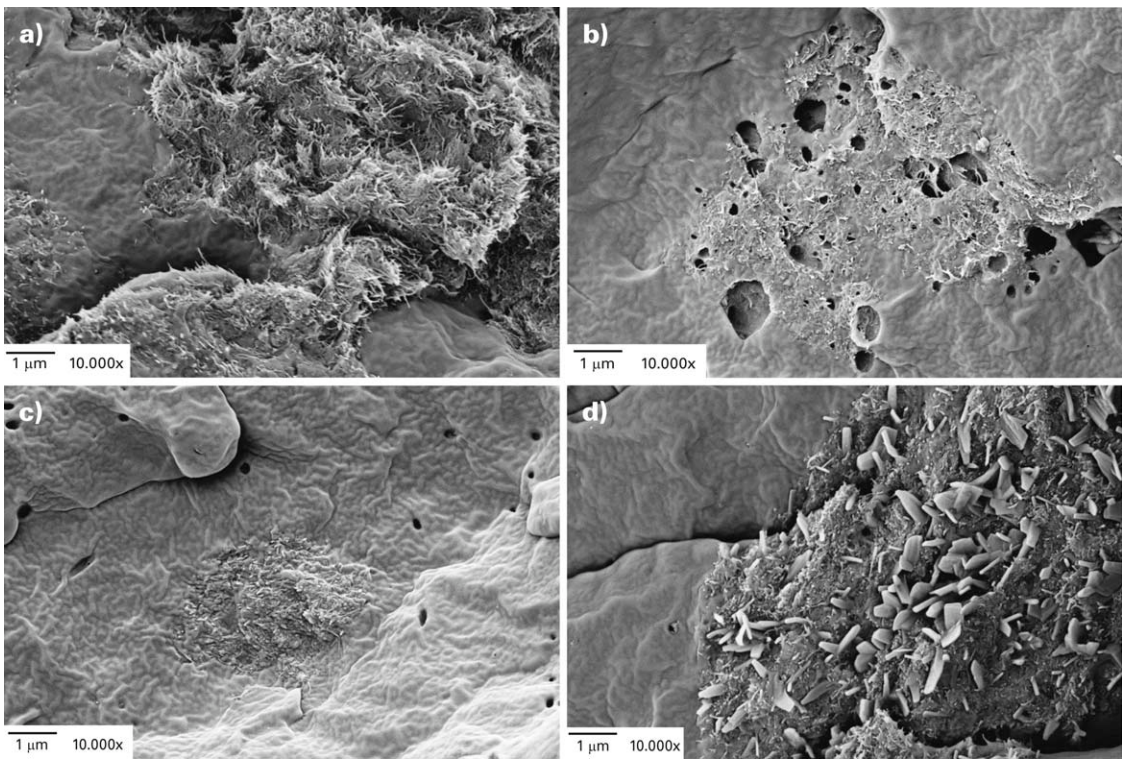

Figure 4 SEM micrographs of fractured surfaces of PP/MWCNT composites: (a) PP/MWCNT, (b) PP/SDS/MWCNT, (c) PP/Brij76/MWCNT, and (d) PP/CTAB/MWCNT.

indicates that a poor wetting by the PP matrix occurred, turning those agglomerates into weak spots and possible sites for failure initiation upon mechanical testing. Further investigation of this sample revealed maximum agglomerate dimensions of up to several hundreds of microns. Figure 4(b) represents the nanocomposites containing MWCNT predispersed in SDS. Here, the size of the agglomerates is considerably smaller than for the sample without any predispersion of the MWCNT. Interestingly, pores in the range of about 1 μm and below can be seen in the vicinity of the MWCNT, similar pictures were obtained at other locations, showing always pores adjacent to the aggregated MWCNT. However, pores well below 1 μm in their dimensions and homogeneously distributed over the fractured surface are observed for the PP/Brij76/MWCNT in Figure 4(c). The characterization by SEM suggests that the predispersion of the MWCNT in Brij76 results in the best distribution homogeneity and lowest agglomerate sizes compared with the other systems. This is likely to be related to the relatively better compatibility of nonionic Brij76 and PP in comparison with anionic SDS-MWCNT. Figure 4(d) shows the fractured surface of the PP/CTAB/MWCNT system. For this system no pores are observed, however, the distribution of the MWCNT is not as homogeneous as for the samples with PP/Brij76/MWCNT and PP/SDS/MWCNT. Moreover, besides the observed MWCNT agglomerates are larger, one can find plate-like structures, which could be the crystallite of CTAB due to its high melting point (mp = 250°C).

Besides the information on MWCNT agglomerate size, the presence of pores in the PP matrix is of interest, as this was not expected. Although the processing temperatures for PP are relatively low compared with other thermoplastic resins, the thermal stability of the surfactants used could account for the observed structures. Figure 5 shows TGA measurement curves for surfactants using dry air as purge gas. The evolution of the relative mass with increasing temperature shows clearly that for all three surfactants a weight loss is observed in the temperature range relevant for the PP processing. Thus, the presence of the pores observed in the SEM micrographs of the fractured surfaces is related to the insufficient thermal stability of the surfactants in air. In the case of the Brij76/MWCNT system, the very homogeneous distribution of the pores in the fractured surface indicates an enhanced distribution of the MWCNT and the surfactant throughout the bulk, whereas in the case of the SDS/MWCNT the appearance of the pores is restricted to larger MWCNT agglomerates. Furthermore, the pores in presence of Brij76 are of very similar appearance showing dimensions of not bigger than 500 nm, whereas in the case of SDS they are considerably

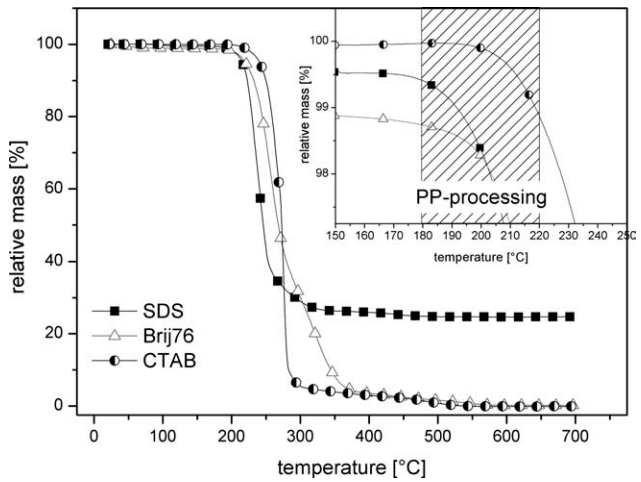

Figure 5 TGA measurements of the surfactants used performed at dry air purge.

bigger and of more irregular shape. The absence of pores in the fractured surface of the MWCNT/CTAB sample is likely to be related to its minor extent of thermal decomposition in the temperature range up to 220°C.

As the DSC measurements were performed on material of the injection molded specimens, it has to be taken into account that the identified change in the nucleating behavior of the MWCNT is related to the surfactants after melt processing.

Tensile properties of the MWCNT/PP nanocomposites

The mechanical characterization of the samples in terms of stress–strain curves and Young's moduli is presented in Figure 6. The shown stress–strain curves for neat PP and the system with the powdery MWCNT show a pronounced reduction in strain at failure for specimens of the latter system. The observed brittleness is a result of the comparably big MWCNT agglomerates acting as sites for crack initiation and preventing the tensile bars from necking as it is observed at larger strains for all other samples. As the results of the tensile properties reflect to a certain degree the distribution homogeneity of the MWCNT in the PP matrix, it becomes evident that the incorporation of the MWCNT in their powdery state into the PP matrix results in the lowest distribution homogeneity, which confirms the observation of SEM. Moreover, this is related to a lower effective surface-to-mass ratio of the MWCNT, which is of importance for nucleation of the PP. However, although a diverging behavior in the strain at failure is observed for the samples with MWCNT-powder, no significant differences in terms of yield stress can be seen. All samples show values of around 30 MPa.

The values for the Young's modulus shown in the inset of Figure 6 indicate the influence of the surfactants and the MWCNT, respectively. Compared with the reference value of the unfilled PP, the addition of powdery MWCNT leads to an increase in the Young's modulus, however, as mentioned before, at the cost of ductility. Moreover, the high standard deviation is evidence for the higher inhomogeneity of this system. The unfilled bars represent the PP/surfactant systems without MWCNT. For the ones with SDS and Brij76 a significant drop in stiffness is observed being more pronounced for the PP/SDS system. In the case of PP/CTAB no significant change with respect to the neat PP is found. Those observations coincide with the details observed in Figure 4. The SDS results in bigger pores than the Brij76, affecting the Young's modulus to a greater extent than the relatively fine pores of the Brij76, whereas for CTAB no pore-like structures could be found leaving the mechanical performance mainly unaffected.

The incorporation of the predispersed MWCNT into the PP causes pronounced changes for the SDS/MWCNT as well as the Brij76/MWCNT system. The reduction in Young's modulus due to the pores is overcompensated by the reinforcing mechanisms inherent to MWCNT, indicating that the state of dispersion for those two systems is considerably better than for the CTAB systems, where the addition of the MWCNT does not cause any significant change in the Young's modulus. However, comparing the absolute values of the systems with the predispersed MWCNT to the unfilled PP, only for the MWCNT/Brij system a modest increase of about 11% is observed, whereas, although slightly higher than for

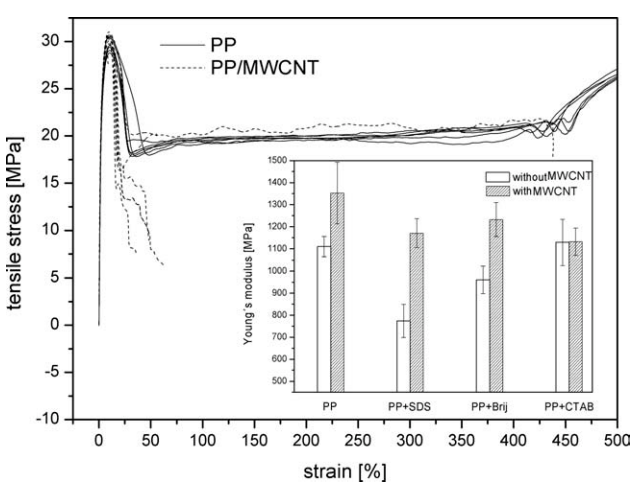

Figure 6 Stress–strain curves of neat PP and PP/MWCNT without surfactant. Inset: Young's modulus of specimens processed with different surfactants and with/without MWCNT.

PP, the change in Young's modulus for the SDS/MWCNT is not significant.

CONCLUSIONS

MWCNT predispersed in presence of various surfactants and incorporated into PP via compounding on a twin-screw extruder followed by injection molding of tensile bars result in different isothermal crystallization behavior and mechanical properties depending on the surfactant used.

The isothermal crystallization of PP is accelerated by all surfactants investigated. However, the surfactants affect the crystallization behavior of PP to a varying extent. Interestingly, the incorporation of powdery MWCNT into the PP without any predispersion resulted in lower crystallization half-time compared with nanocomposites based on Brij76/MWCNT and CTAB/MWCNT, although the latter ones showed a superior distribution of the MWCNT. This indicates that the surfactant molecules adsorbed onto the MWCNT surface remain in the PP/MWCNT interface after melt processing, affecting the nucleation ability of the MWCNT. Hence, the contribution to the nucleation of the PP by the surfactants and MWCNT, respectively, can not be regarded separately as the nucleating ability of the MWCNT is lowered by the adsorbed surfactants.

Although surfactants serve as efficient dispersants for CNT, it could be shown that their application in melt processing of thermoplastic can cause thermal degradation upon contact with the ambient environment in combination with elevated temperatures. This is revealed by TGA measurements as well as the observation of pores in the fractured surfaces of the nanocomposites. The effect of pores was reflected in a decay of the Young's modulus for the systems PP/SDS and PP/Brij76 system, respectively. The presence of the predispersed MWCNT can make up for the lower stiffness induced by the pores, resulting in slightly higher values for the Young's modulus than in the case of the unfilled PP.

The authors would like to thank Dr. R. Häßler, S. Görner, C. Scheffler, and R. Koch for experimental assistance.

References

1. Iijima, S. Nature 1991, 354, 56.
2. Coleman, J. N.; Khan, U.; Blau, W. J.; Gun'ko, Y. K. Carbon 2006, 44, 1624.
3. Du, J. H.; Bai, J.; Cheng, H. M. Express Polym Lett 2007, 1, 253.
4. Villmow, T.; Pegel, S.; Pötschke, P.; Wagenknecht, U. Compos Sci Technol 2008, 68, 777.
5. Alig, I.; Lellinger, D.; Engel, M.; Skipa, T.; Pötschke, P. Polymer 2008, 49, 1902.
6. Valentino, O.; Sarno, M.; Rainone, N. G.; Nobile, M. R.; Ciambelli, P.; Neitzert, H. C.; Simon, G. P. Phys E 2008, 40, 2440.
7. Thess, A.; Lee, R.; Nikolaev, P.; Dai, H.; Petit, P.; Robert, J.; Xu, C.-H.; Lee, Y.-H.; Kim, S.-G.; Rinzler, A. G.; Colbert, D. T.; Scuseria, G. E., Tománek, D.; Fischer, J. E.; Smalley, R. E. Science 1996, 273, 483.
8. Pegel, S.; Pötschke, P.; Petzold, G.; Alig, I.; Dudkin, S. M.; Lellinger, D. Polymer 2007, 49, 974.
9. Ganß, M.; Satapathy, B. K.; Thunga, M.; Weidisch, R.; Pötschke, P.; Jehnichen, D. Acta Mater 2008, 56, 2247.
10. Grossiord, N.; Regev, O.; Loos, J.; Meuldijk, J.; Koning, C. E. Anal Chem 2005, 77, 5135.
11. Matarredona, O.; Rhoads, H.; Li, Z.; Harwell, J. L.; Balzano, L.; Resasco, D. J Phys Chem B 2003, 107, 13357.
12. Yu, J.; Grossiord, N.; Koning, C. E.; Loos, J. Carbon 2007, 45, 618.
13. Huang, W.; Lin, Y.; Taylor, S.; Gaillard, J.; Rao, A. M.; Sun, Y. Nano Lett 2002, 2, 231.
14. Miltner, H. E.; Grossiord, N.; Lu, K.; Loos, J.; Koning, C. E.; van Mele, B. Macromol 2008, 41, 5753.
15. Valerie, C.; Moore, M.; Strano, S.; Haroz, E. H.; Hauge, R. H.; Smalley, R. E. Nano Lett 2003, 3, 1379.
16. Gao, S. L.; Mäder, E.; Plonka, R. Acta Mater 2007, 55, 1043.
17. Mäder, E.; Rausch, J.; Schmidt, N. Compos A 2008, 39, 612.
18. Strano, M. S.; Moore, V. C.; Milter, M. K.; Allen, M. J.; Haroz, E. H.; Kittrell, C.; Hauge, R. H.; Smalley, R. E. J Nanosci Nanotechnol 2003, 3, 81.
19. Kataura, H.; Kumazawa, Y.; Maniwa, Y.; Umezu, I.; Suzuki, S.; Ohtsuka, Y.; Achiba, Y. Synth Met 1999, 103, 2555.
20. O'Connell, M. J.; Bachilo, S. M.; Huffman, C. B.; Moore, V. C.; Strano, M. S.; Haroz, E. H.; Rialon, K. L.; Boul, P. J.; Noon, W. H.; Kittrell, C.; Ma, J.-P.; Hauge, R. H.; Weisman, R. B.; Smalley, R. E. Science 2002, 297, 593.
21. Yurekli, K.; Mitchell, C. A.; Krishnamootri, R. J Am Chem Soc 2004, 126, 9902.
22. Grossiord, N.; van der Schoot, P.; Meuldijk, J.; Koning, C. E. Langmuir 2007, 23, 3646.
23. Gong, X.; Liu, J.; Baskaran, S.; Voise, R. D.; Young, J. S. Chem Mater 2000, 12, 1049.
24. Rausch, J.; Zhuang, R. C.; Mäder, E. Composites A, submitted.
25. Grady, B. P.; Pompeo, F.; Shambough, R. L.; Resasco, D. E. J Phys Chem B 2002, 106, 5852.
26. Assouline, E.; Lustiger, A.; Barber, A. H.; Cooper, C. A.; Klein, E.; Wachtel, E.; Wagner, H. D. J Polym Sci: Part B Polym Phys 2003, 41, 520.
27. Zhou, Z.; Wang, S.; Lu, L.; Zhang, Y.o; Zhang, Yi. J Polym Sci: Part B Polym Phys 2007, 45, 1616.
28. Avila-Orta, C. A.; Medellin-Rodriguez, F. J.; Davila-Rodriguez, M. V.; Aguirre-Figueroa, Y. A.; Yoon, K.; Hsiao, B. S. J Appl Polym Sci 2007, 106, 2640.
29. Bhattacharyya, A. R.; Sreekumar, T. V.; Liua, T.; Kumara, S.; Ericson, L. M.; Hauge, R. H.; Smalley, R. E. Polymer 2003, 44, 2373.
30. Leelapornpisit, W.; Ton-That, M. T.; Perrin-Sarazin, F.; Cole, K. C.; Denault, J.; Simard, B. J Polym Sci: Part B Polym Phys 2005, 43, 2445.
31. Seo, M. K.; Lee, J. R.; Park, S. J. Mater Sci Eng A 2005, 404, 79.
32. Avrami, M. J Chem Phys 1939, 7, 1103.
33. Lorenzo, A. T.; Arnal, M. L.; Albuerne, J.; Müller, A. J. Polym Test 2007, 26, 222.